Experimental characterisation of damped CFRP materials with an application to a lightweight car door

Alessandro Fasana[1], Alessandro Ferraris[3], Andrea Giancarlo Airale[4], Davide Berti Polato[5] and Massimiliana Carello[2]
[1]Politecnico di Torino, Italy, e-mail: alessandro.fasana@polito.it
[3]Politecnico di Torino, Italy, e-mail: alessandro.ferraris@polito.it
[4]Politecnico di Torino, Italy, e-mail: andrea.airale@polito.it
[5]Politecnico di Torino, Italy, e-mail: davide.bertipolato@polito.it
[2]Politecnico di Torino, Italy, e-mail: massimiliana.carello@polito.it

Abstract. This paper presents a complete design procedure for defining a dynamic model of a Carbon Fibre Reinforced Polymer (CFRP) component with an embedded damping material layer. The experiment to determine the mechanical characteristics of the materials is performed by the Oberst beam technique to provide precise material properties for a Finite Element (FE) model. The technique implemented, namely the Linear Identification by Polynomial Expansion in the Z-domain (LIPEZ) method, is used to compare the experimental data with the numerical simulation results provided by the modal parameters to be compared with the numerical results. Two automotive components (a leaf spring and an outer shell of front door) have been tested. The research revealed the utter importance of a correct definition of the geometry for the numerical models. Finally, the positive effects for acoustic performance with a thin layer of KRAIBON® SUT9609/24 damping material, included in the stacking sequence of the CFRP component, are highlighted.

Keywords: CFRP characterization, experimental modal analysis, FEM, constrained damping material, damped CFRP car door.

1 Introduction

Recently, car buyers have risen their expectation on vehicle comfort with respect to the past, when performances and reliability were sufficient to set the quality of the vehicles. Vehicle electrification in this contest emphasize the Noise and Vibration Harshness (NVH) because of the absence of the thermal engine noise and the more widely use of lightweight material [1], [2], [3], [4]. Carbon fibre reinforced plastic (CFRP) materials provide good mechanical characteristics and promote light structures but emphasized NVH at the same time. For this reason, the use of damping materials in passive constrained layer configuration is often taken into consideration [5] to lower the vibrational response of CFRP structures, but such procedure increases both the weight and the manufacturing process. A precise numerical model, e.g. a finite element model (FEM) of a structure is only reliable if material properties are correctly defined, so that Section 2 deals with the use of the so-called Oberst test method [6]–[8] to define Young modulus, loss factor of damping and structural materials. These properties have been calculated through the analysis of the frequency response of tested samples, measured at different temperatures in controlled climatic condition. As expected, the CFRP properties do not change whilst the damping material and the result shows a quite typical viscoelastic behaviour.

With the aim of defining a complete design procedure for CFRP (automotive) components with an embedded damping layer, the comparison of the numerical (from a FEM) and the measured mode shapes (from experimental modal analysis) is the most feasible and diffused procedure [9], [10]. Over the last few decades, a number of papers dealing with the problem of modal parameters estimation of vibrating structures has been presented, [11]–[13] are good examples. The linear identification by polynomial expansion in the Z-domain (LIPEZ) method adopted in this paper starts from the rational fraction polynomials (RFP) representation of the frequency response function (FRF) and expounds a total least square method in the Z-domain [14]. The procedure is briefly presented in Section 3. In particular, the method is applied [15] to two automotive components which are also reproduced at simulation level with computational FEM simulation in order to perform a correlation analysis. The chosen components include a leaf spring (Section 4) with simple geometry, and a door panel (Section 5) for its influence in vehicle global NVH characteristics. Both components are made with structural CFRP, whose mechanical properties has been examined in Section 2 using the Oberst beam test method.

2 CFRP and damped sandwich characterization

This section describes the procedure adopted to measure the Young's modulus and the loss factor of two different materials: a set of pure T300 epoxy, twill CFRP [0/90/0] specimens and a set of 5 layers sandwich specimens with the following staking sequence [0/90] CFRP + 1 Layer KRAIBON® SUT9609/24 + [0/90] CFRP structure combining interlaminar damping material with 2 layers of CFRP T300. The activity aims at defining the characteristics of the materials, which is going to be introduced in the material card of a FE simulation.

The Oberst beam test is a standard method [6] to characterise laminated materials and basically consist in a clamped-free beam as shown in Figure 1. The beam is excited by a contactless electromagnetic transducer, which exerts a swept-sine force. The input force frequency range depends on the type of specimen under test. Another contactless capacitive transducer is located at the tip of the beam to detect the output response (velocity): the spectrum of the output identifies the natural frequencies of the beam and its loss factor. In its simplest form the identification procedure is based on the -3dB method (or half-power method), but more objective results can be achieved by implementing a least square fitting of the spectrum. By analysing the natural frequencies with Bernoulli-Euler beam model the Young's modulus can be determined.

Tests have been performed in a thermally controlled environment at different temperatures, from -20 °C to +60°C with steps of 10 °C. The first natural frequency has always been discarded, since it can be too much affected by the imperfect constraint conditions [2]. Three samples of each material have been aged for (250, 500 and 750 h) and then tested to establish the effect of aging on damping capabilities of the interlaminar material. Table 1 gives the mean characteristics of the three samples, while Figure 2 presents the average variation of Young's modulus and loss factor with frequency. The CRFP T300 (Figure 2) has very stable properties and very low damping (<1%) while the sandwich configuration – CFRP T300 + KRAIBON® SUT9609/24 (Figure 3) – shows the typical variations of viscoelastic materials and very good damping in the whole temperature range 0-30 °C.

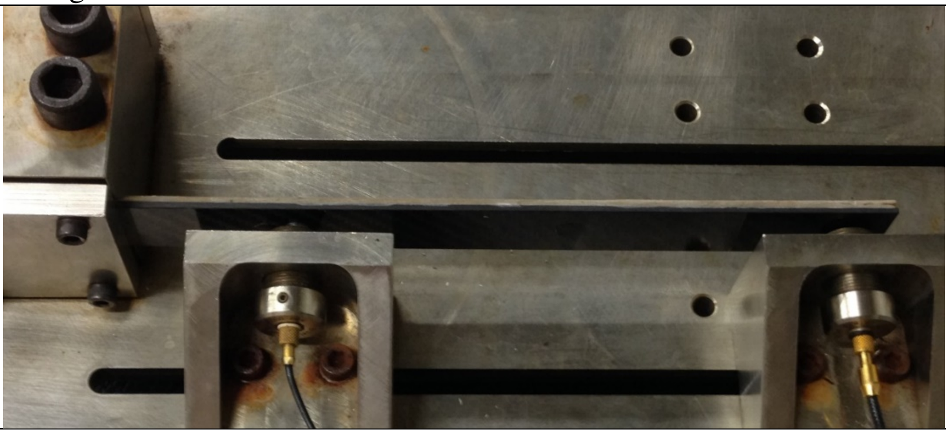

Figure 1: The Oberst beam test bench.

Table 1: Mean characteristics of the samples

Sample	Layers	Thickness (mm)	Length (mm)	Mass (kg)	Density (kg/m^3)
CFRP T300	3	0,91	259,88	0,00393	1305
KRAIBON® SUT9609/24	3+1+3	1,72	259,75	0,0074	1308

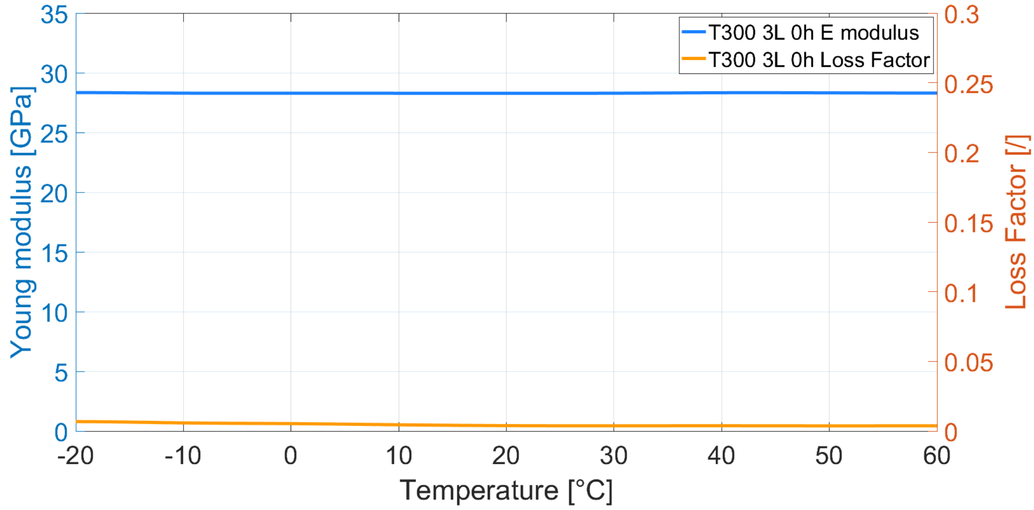

Figure 2: Material characteristics as a function of temperature: CFRP T300 material

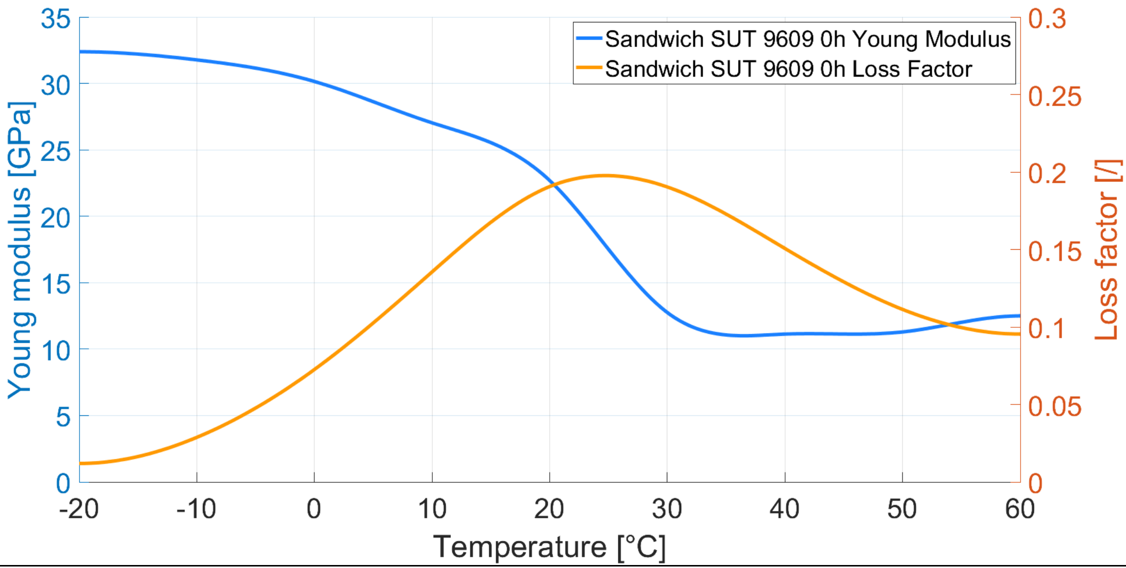

Figure 3: Material characteristics as a function of temperature: T300 + KRAIBON® SUT9609/24 sandwich

The definition of the mechanical properties of these materials paves the way to their application to two test cases: a CFRP leaf spring and a CFRP car door panel - with or without a damping material in the constrained layer configuration. The numerical results obtained by a FEM have been compared to experimental results in terms of natural frequencies and mode shapes, extracted by the LIPEZ method.

3 Outline of the LIPEZ method

The LIPEZ method is a frequency domain modal parameter extraction technique, which takes advantage of the Z-transform formulation. The procedure is briefly summarized in this section but its complete description is found in [10].

For a linear and time invariant system with n degrees of freedom, the FRF can be expressed by:

$$H_k = \sum_{r=1}^{2n} A_r \frac{z_k}{z_k - z_r} \tag{1}$$

Where: $H_k = H(\Omega_k)$ is the generic spectral line of the FRF, evaluated at frequency:

$$\Omega_k = (k-1)\Delta\Omega = (k-1)2\pi\Delta f = \pi f_s (k-1)/(N-1) \tag{2}$$

Where: f_s is the sampling frequency, Δf is the frequency resolution, N is the number of spectral lines and k = 1... N.
The terms related to the Z-transform are:

$$z_r = e^{s_r \Delta t} \tag{3}$$

$$z_k = e^{i(k-1)\Delta\Omega\Delta t} = e^{i\pi(k-1)(N-1)} \tag{4}$$

Where: $i = \sqrt{-1}$ and the poles s_r are linked to the natural angular frequencies ω_r and damping ratios ξ_r by the expression $s_r = -\xi_r\omega_r + i\omega_r\sqrt{1-\xi_r^2}$.
The sum in Eq. (1) can be converted in the following rational fraction expression:

$$H_k = \frac{b_1 z_k + \cdots + b_{2n} z_k^{2n}}{a_0 + a_1 z_k + \cdots + a_{2n-1} z_k^{2n-1} + z_k^{2n}} \tag{5}$$

where the 4n unknown coefficients $a_0, \ldots, a_{2n-1}$ and $b_1, \ldots, b_{2n}$ are real valued. Eq. (5) can be written for N spectral lines and for many FRFs (namely NFRF) to get an overdetermined linear system of equations:

$$\begin{bmatrix} \mathbf{A_1} \\ \vdots \\ \mathbf{A}_{NFRF} \end{bmatrix} \mathbf{a} + \begin{bmatrix} -\mathbf{B} & \cdots & \mathbf{0} \\ \vdots & \ddots & \vdots \\ \mathbf{0} & \cdots & -\mathbf{B} \end{bmatrix} \begin{Bmatrix} \mathbf{b_1} \\ \vdots \\ \mathbf{b}_{NFRF} \end{Bmatrix} = \begin{Bmatrix} \mathbf{w_1} \\ \vdots \\ \mathbf{w}_{NFRF} \end{Bmatrix} \tag{6}$$

where $\mathbf{a} = [a_0\ a_1\ \cdots\ a_{2n-1}]^{\boldsymbol{T}}$ and $\mathbf{b_m} = [b_1\ b_2\ \cdots\ b_{2n}]_{\boldsymbol{m}}^{\boldsymbol{T}}$ (*m=1,..., NFRF*) are the vectors to be determined. The matrix in Eq. (6) can surely be solved but the procedure can be time consuming, especially when large data sets are analyzed (NFRF>>1) and n has to vary (e.g. to define a stabilization chart). A much quicker least square procedure can indeed be implemented to limit, at first, the solution to vector **a**:

$$\mathbf{Ra} = \mathbf{r} \tag{7}$$

The real, square (2n×2n) and well-conditioned matrix **R** contains the information of all the measured FRFs but a system of only 2n equations has to be solved. The poles $s_r = \ln z_r / \Delta t$ can then be obtained by using the equation:

$$a_0 + a_1 z + \cdots + a_{2n-1} z^{2n-1} + z^{2n} = 0 \tag{8}$$

Any vector $\mathbf{b}_m$, the related modal constants A_r and eventually the mode shapes, can then be recovered from Eq. (5).
An *open source* version of the implemented method can be obtained from the authors under the CC BY license.

4 Leaf spring application

This section is devoted to the comparison of the numerical simulation and experimental results of a CRFP leaf spring formed by 31 layers of Epoxy CFRP T300, twill 2x2 240 gr/m^2, following the stacking sequence $[0/(0/45)_{14}/\ 0/0]$.

4.1 Experimental tests

The test aims at computing the modal parameters of the system in the free–free condition, with the component vertically suspended by elastic supports as shown in Figure 4, or by a Single Point Constrain (green in Figure 5). The leaf spring was excited by an electromagnetic shaker, driven by a white noise input signal in the frequency range 2–1000 Hz. A 24 channels signal acquisition board (OROS OR38) was used to simultaneously record the responses of 23 piezoelectric accelerometers (outputs) and the force, actuation force is delivered to the beam by a load cell positioned in the right bottom corner. Considering the leaf spring dimensions, one set of properly distributed accelerometers is sufficient to investigate the vibrational behaviour of the component.
Time domain input (force) and output (acceleration) data have been processed according to the Hv estimator [16] to produce the FRFs, which are the required inputs for the LIPEZ method. The coherence functions (not reported here for the sake of brevity) confirm the validity of the experimental setup, showing local minima much lower than one only at resonances and anti-resonances. Also the input spectrum is reasonably flat, except near resonances. All data can be obtained from the authors.

Figure 4: The leaf spring component: The experimental configuration with 23 accelerometers

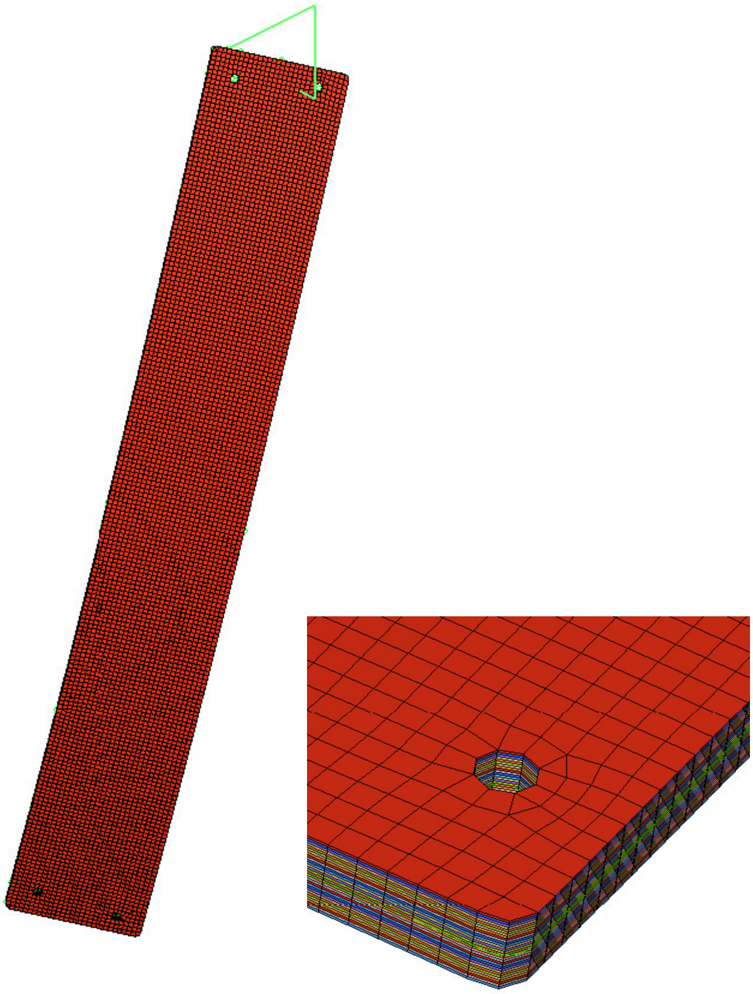

Figure 5: The leaf spring component: The finite element model, with a detailed view.

The unknown model order n, i.e. the number of modes, is increased from a minimum to a maximum value (1-25) and the results are plotted in stabilization charts: Figure 6 and Figure 7 present the stabilization diagrams of natural frequencies and damping ratios, overlaid on the sum of the moduli of all FRFs. Separating physical from computational modes is very simple as very stable frequency lines can be observed in Figure 6. A slight scatter of damping ratios is observed in Figure 7, but the modal damping is always very low ($< 0.5\%$).

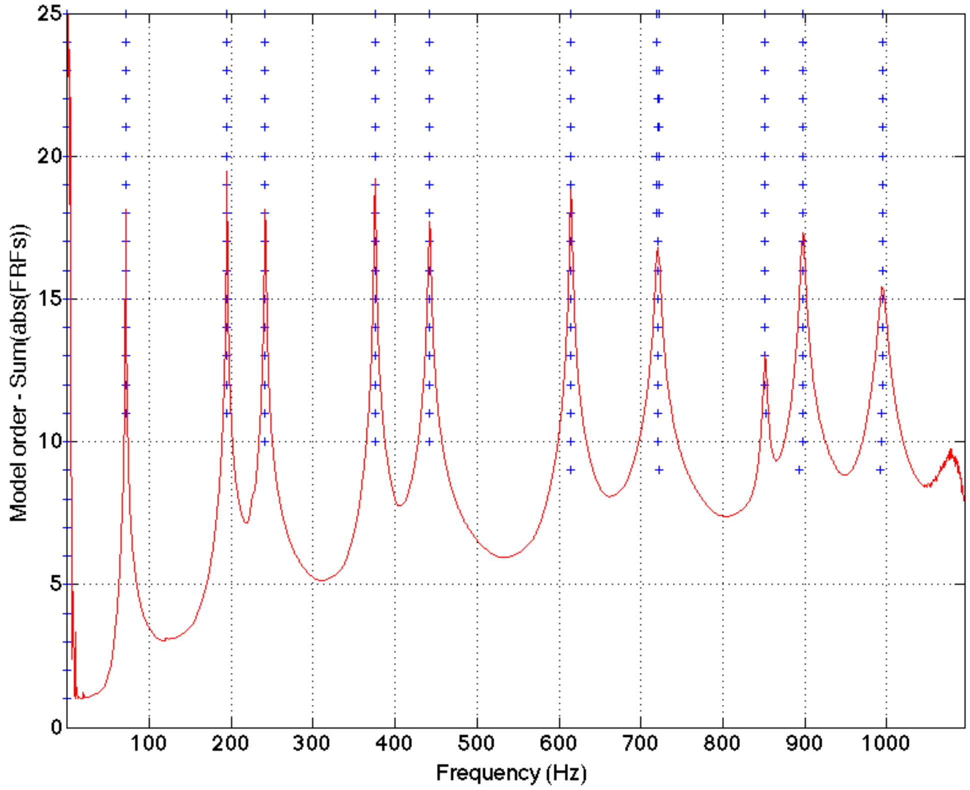

Figure 6: Stabilization diagram for the natural frequencies. Each " + " corresponds to an estimated frequency in the selected band, given the model order n (ranging from 1 to 25).

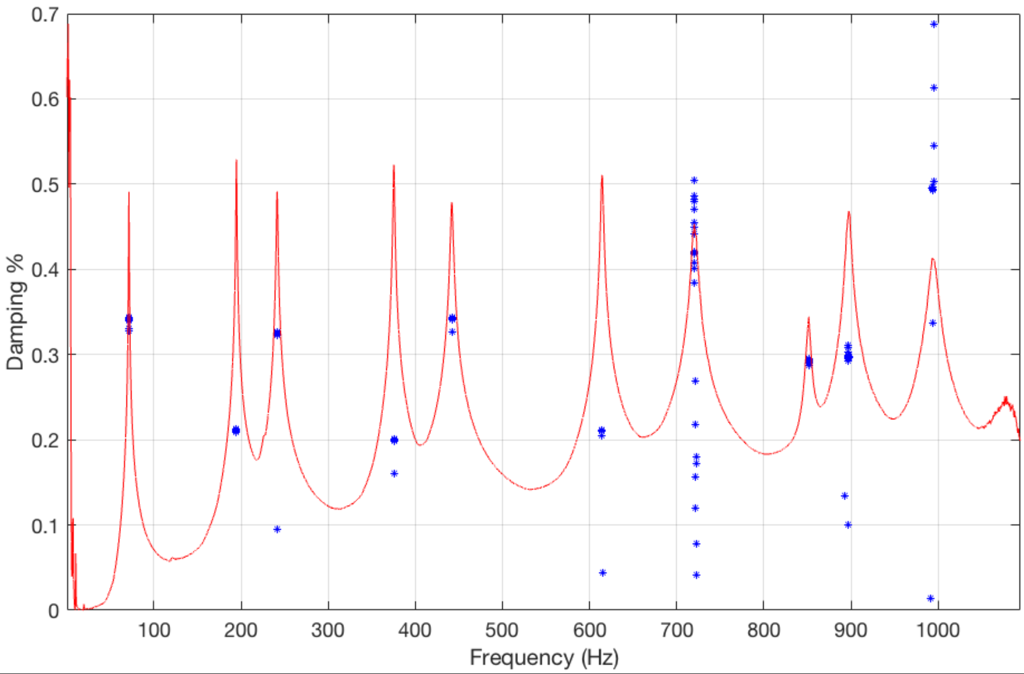

*Figure 7: Stabilization diagram for the damping ratios. Each " * " corresponds to a pair natural frequency – damping ratio, given the model order n (ranging from 1 to 25). For some modes, e.g. mode 2 at about 200 Hz, many points are almost completely superimposed.*

4.2 Finite element model

The simple geometry of the item and the detailed characterisation of the material properties – described in Section 2 – allowed to define an accurate FE model by using Altair Hypermesh (Optistruct® implicit solver) as specified in[17], [18]. The FE model precisely takes into account the stacking sequence and orientation of the plies of the actual leaf spring, whose production process was strictly controlled in all its steps from the selection of the materials to the final curing of the component. The 31 plies of CFRP have been modelled as a composite laminate by using the "PCOMPP" property card and the material card "MAT 8". The property is chosen because it gives the possibility to characterize layer by layer the laminate, defining the stacking sequence, thickness, material and orientation of each layer. The material card has been chosen because is the only one dedicated for PCOMPP property which permit the implementation of orthotropic characteristics for shell elements as defined in [17] and [18]. Material characteristics implemented in the virtual model are defined as follows:

- Young modulus $E_1 = E_2 = 44700$ MPa;
- $G_{12}= 2500$ MPa;
- Poisson ratio $\upsilon_{12} = 0.03$;
- Density $\varrho = 1460$ kg/m^3;
- Loss factor $\eta = 0.047$.

The component is meshed with about 7000 shell elements, with mean shell size of 5 mm, which well subdivide the entire surface of the component. The elements dimension has been properly defined by means of convergence test, not reported for sake of brevity [19]. Shell elements has been chosen because of model complexity reduction considering that stresses distribution along the thickness can be neglected. No constraints are applied to the model to simulate a free-free condition replicating the real test.

It's important to point out that the first six vibrating modes (at almost zero frequency) describe the rigid body motion and are not be taken into account in the following analysis.

The Lanczos algorithm [20], [21] has been used to solve the undamped eigenvalue problem; the damping matrix is disregarded not only for limiting the numerical issues, but also because as proven by the Oberst beam test and the experimental modal analysis, the damping capability of the CFRP is in fact very limited. The damping matrix should anyway be simply described by the proportional damping model because in this configuration damping can be attributed to the inherent properties of the material.

4.3 Comparison

To evaluate the correlation between the numerical analysis and the experimental results, the Modal Assurance Criterion (MAC) is adopted as described in [5, 6]:

$$MAC_{TS} = \frac{\left|\{\psi_N\}^T\{\psi_E\}^*\right|^2}{(\{\psi_N\}^T\{\psi_N\}^*)(\{\psi_E\}^T\{\psi_E\}^*)} \tag{8}$$

Where $\{\psi_N\}$ and $\{\psi_E\}$ indicate numerical and experimental mode shapes respectively. This index indicates the similarity between the modes shapes and is equal to one when two compared modes have exactly the same shape. Figure 8 gives a pictorial representation of the MAC matrix, while Table 2 presents the numerical values on the main diagonal. It can be noticed that the minimum value is a very good (0.84 for the first 10 analysed modes). The same Table also lists the experimental and numerical natural frequencies, showing a quite good correlation. As expected, modal damping ratios are very limited.

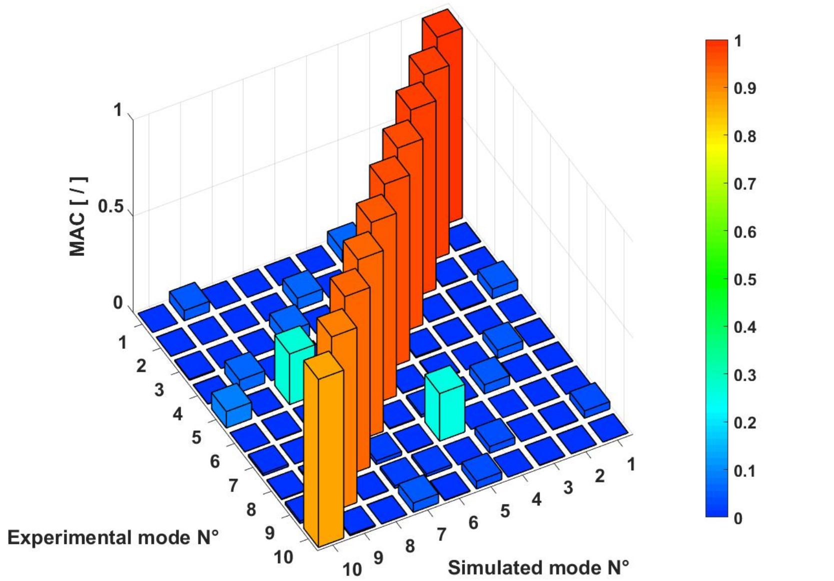

Figure 8: MAC coefficient for the leaf spring test

Table 2: Natural frequencies, damping ratios and MAC values for the leaf spring.

Mode number	f_N (Hz)	f_E (Hz)	Δf (%)	ζ_E	diag(MAC)
1	67,80	71,3	-4,9	0.34	0,98
2	188,4	194,7	-3,2	0,21	0,97
3	238,3	241,4	-1,3	0,32	0,97
4	370,8	375,4	-1,2	0,20	0,96
5	452,4	442,0	2,6	0,34	0,96
6	614,6	614,4	0,0	0,21	0,95
7	748,8	720,2	4,0	0,38	0,93
8	828,3	851,6	-2,7	0,29	0,84
9	919,8	897,4	2,5	0,30	0,91
10	1053,9	994,5	6,0	0,49	0,87

This first experiment validates the five steps of the design procedure:
1) Characterize the materials;
2) Carefully control the production of the component, especially the orientation of the fibres;
3) Build a FEM which precisely reproduce the actual geometry and stacking sequence;
4) Experimentally extract the modal parameters;
5) Compare the model with the experimental results.
All of these steps are necessary to fulfil the request of a reliable model, as clearly pointed out by the example described in the following chapter.

5 Car door case

The same design procedure has been followed on a more sophisticated test case: a CRFP car door panel.
In modern light weight design for vehicles, doors are formed by two separately produced thin shells of CFRP material, which are then tightly bonded along their outer borders. The final structure is extremely lightweight, but because of its relatively large and flat flexible surface, the influence on the acoustic characteristics of the vehicle is significant. In order to decrease the sound emission of the structure, a thin layer of damping material has been inserted along the stacking sequence, mainly for two reasons: first of all, it has to be stressed that the

thin damping material is positioned on the same mould as the other carbon fibre layers and undergoes the same curing process as the standard CFRP material. A single (proper) production sequence has to be performed for both the CF and the damping layers so that, after curing the two separated panels, there is no need to handle again the two shells and the total cost can be reduced. The second reason is that the increment of the damping properties of the assembly is more controllable, because the constrained layer solution (CFRP-damper-CFRP) performs much better than the free layer solution (CFRP-damper).
In this section the comparison of numerical and experimental results of the external shell of a door panels are presented with or without the integrated damping material layer.

5.1 Experimental tests

The external shell of the door was tested in free – free conditions, with a white noise excitation force given through an electromagnetic shaker. Again, 23 accelerometers and a load cell were used to record the response but in this case two repetitions were needed to measure 44 points, aiming at a good mode shapes definition (Figure 9). The load cell was fixed on the left bottom corner and a white noise excitation was generated in the 0-400 Hz band. The procedure followed for data acquisition is the same as for the leaf spring and again coherence remain almost equal to one in all the analysed frequency range, thus confirming the quality of the measured data.
Some spurious (numerical) modes are extracted by the LIPEZ method and they were simply detected by checking the stabilization diagram of damping ratios (Figure 9): numerical and non-acceptable solutions correspond to unstable or unrealistically high damping ratios, e.g. the values in the 8-16 Hz band in Figure 10.
The modal parameters extraction has been limited to the frequency range 4 – 130 Hz which contains 11 modes.

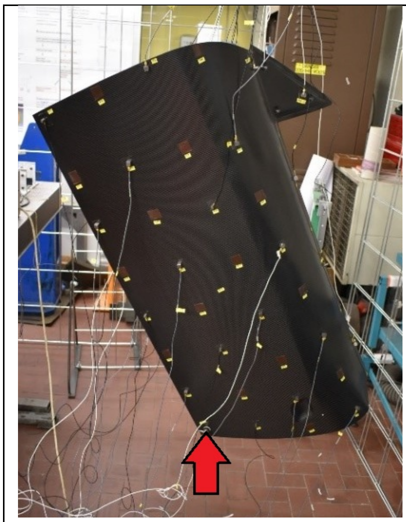

Figure 9: The door panel: Experimental configuration with 23 accelerometers, a load cell (red arrow) and 44 measurement points;

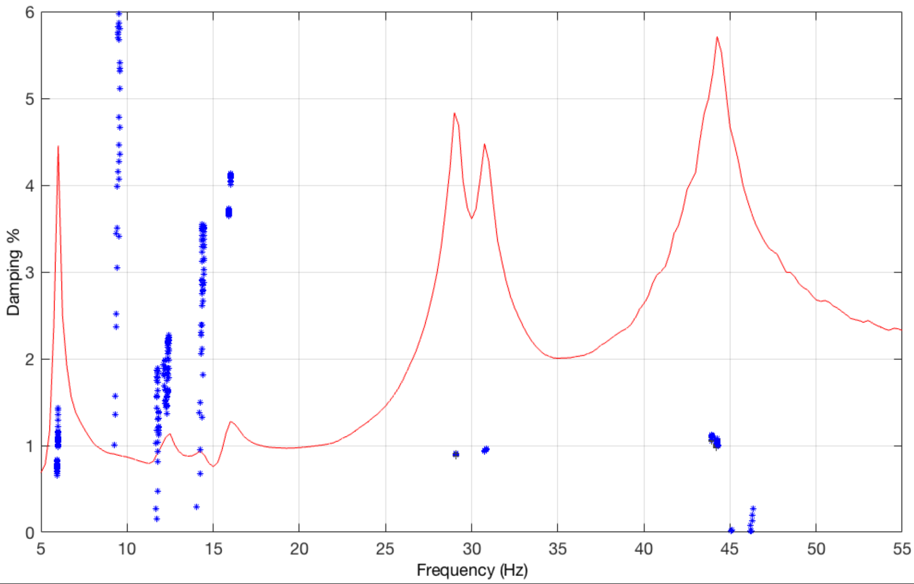

*Figure 10: The door panel: Stabilization diagram for the damping ratios: each " * " corresponds to a pair natural frequency – damping ratio.*

5.2 Finite element model

The shell of the door panel is a handmade component of CFRP layers but its production model has been quality controlled, to ensure an actual orientation of the fibres as accurate as possible. Also the thickness of the shell

has been carefully measured to limit the undesired uncertainty which could occur in proximity of small curvature radii.
The FE models are defined to reproduce the real components, with the same materials described in Section 2. A summary of the FEM main characteristics follows:

- CFRP T300 material;
- Orthotropic CFRP laminate, $[0/90]_3$;
- Free - free condition (no model constraints);
- Element type: shell;
- Maximum mesh size: 4 mm;
- Eigenproblem solver: Lanczos algorithm.

5.3 Comparison

The visual comparison, confirmed by the values of the MAC matrix and the natural frequencies, shows a really poor agreement between numerical and experimental mode shapes. For example, Figure 11 gives a graphical representation of the MAC matrix, which is disappointing.
Since the material has been characterized according to the procedure described in Section 2 (which lead to an excellent model for the leaf spring) and the experimental results are very stable and reliable, the issue may be related to the aspect that does not match the requirements of the design sequence listed in Section 4.3.
The ideal disposition of the CF layers has accurately been respected at the production stage and later reproduced by the FE model, but the geometry was obtained by a sort of “reverse engineering” process. Unfortunately, a complete mathematical model of the mould is not available so that its surface has been scanned by a laser. The measured points form a basis for the ensuing CAD representation which, in turn, is the basis for the FE model. It is then reasonable to attribute the differences between numerical and experimental results to an inaccurate geometry of the FE model. A detailed revision of the numerical model has then been carried out, with particular attention to a correct definition of the curvature of the panels. The macroscopic difference is almost negligible, for example the mass variation is limited to a mere 0.14% but the refinement is essential to tune the dynamic properties of the model and cope with the experimental results. The MAC matrix represented in Figure 12 is still not as good as expected but at least for the first four modes the coefficients (main diagonal) are above 90%, confirming the impression given by the visual inspection of the mode shapes (Figure 13). Differences are still present and can be attributed to both experimental and numerical issues: the numerically redesigned geometry is not perfect yet, the orientation of the carbon fibres is not completely identical to the real components (the CFRP door panel is made by warping the fabricant on the mould, orientation is complicated for surface with corners), the directions assigned to the measured accelerations (which are used to define the 3D mode shapes on the basis of the identified eigenvectors $\{\psi_E\}$) have inaccurately been measured, the mass of accelerometers, load cell and cables is not negligible with respect to the structure and also moves the system away from the ideal free-free conditions.
The conclusion is that the exact definition of the geometry and the disposition of the fibres is compulsory for a correct simulation of the dynamic behaviour of such extended and lightweight structures. The simple check on the weight of the component and its qualitative visual examination are not sufficient to accept the model, even if it is apparently very simple.

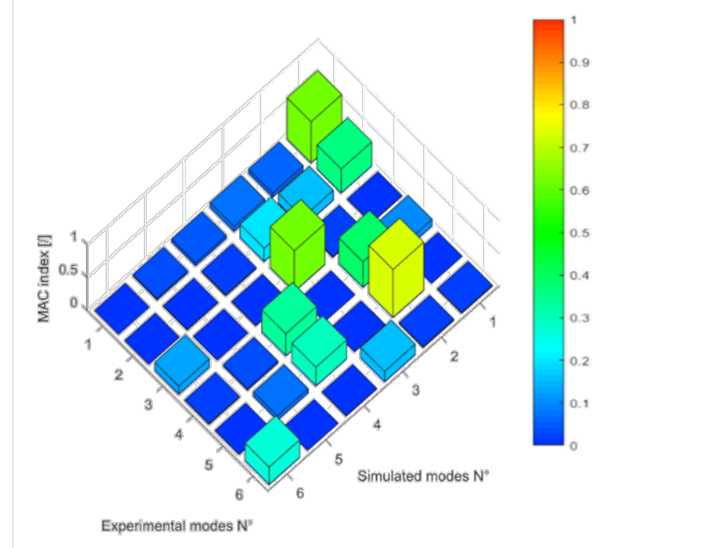

Figure 11: MAC coefficient for the door test, before geometry refinement

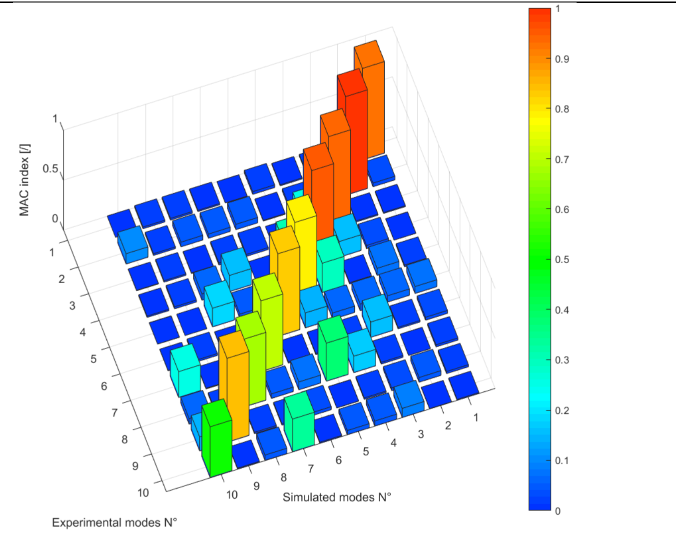

Figure 12: MAC coefficient for the door test, after geometry refinement

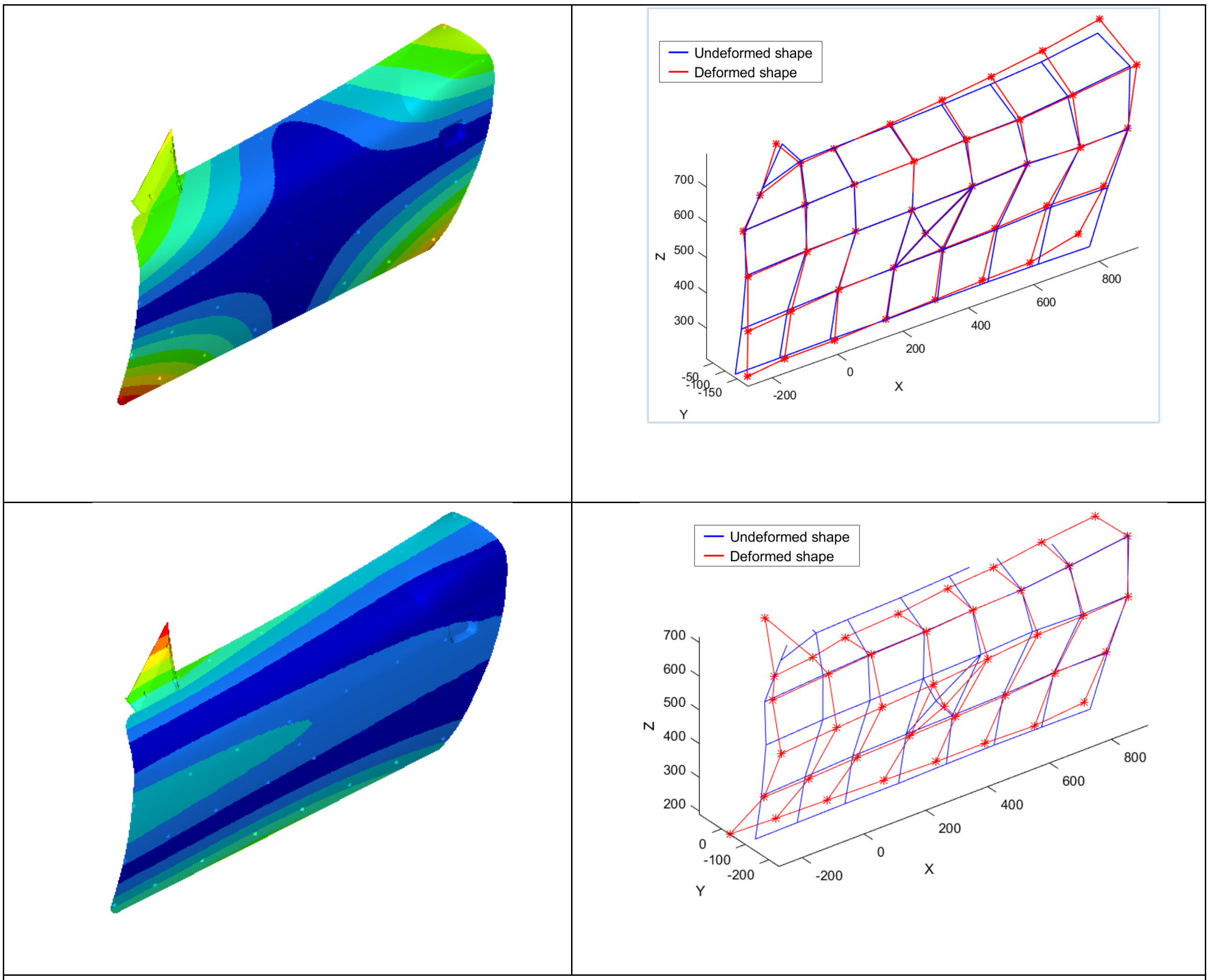

Figure 13: The first two mode shapes after the geometry refinement; left: FEM; right: experimental

5.4 Damped vs undamped configuration

This section compares the FRFs of the external shell of the door with and without an embedded layer of damping material. The original shell is formed by six CF layers, with total mass equals to 2.09 kg, which are almost unable to dissipate vibration energy as pointed out by the low values modal damping ratios (about 1%, see Figure 10). A similar shell has been manufactured (same material, same orientation of the fibres) with a 3-1-3 stacking sequence: the inner core is a made of a KRAIBON® SUT9609/24 damping layer which undergoes the same curing cycle as the CFRP. The SUT9609/24 damping material is divided in two patches as sketched in Figure 14 and the total mass of the damped door is 2.24 kg, a very limited increment with respect to the undamped configuration.

The two shells underwent the same experimental tests and 44 FRFs were measured (see Figure 9) by using a random input in the band 0-400 Hz. The effect of the damping material is obvious when listening to the sound emitted by the two panels (undamped & damped). A quantification of the effectiveness of the constrained layer is given in Figure 15 where the sum of the moduli of all 44 FRFs (inertance) is plotted: the red dotted line (no damping) is well above the solid blue curve along the entire testing frequency range, especially for frequency higher than 50 Hz (which is important for limiting the interior noise harshness).

Table 3 gives the overall value of the FRFs, i.e. the sum of the modals extended over a certain frequency range, for the two configurations. Even in the 0-100 Hz region the difference is above 3dBs, i.e. half-power, and furtherly increases with the frequency band.

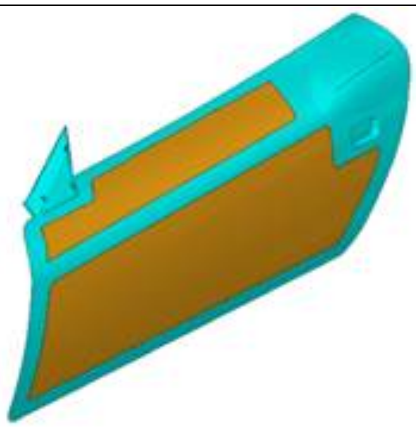

Figure 14: Comparison of the damped and undamped panels: Position of the damping patches;

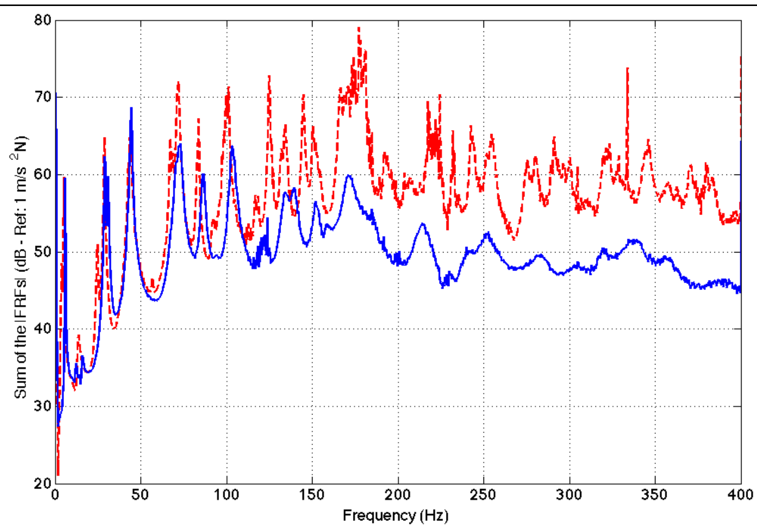

Figure 15: Comparison of the damped and undamped panels: Sum of the FRFs: red dashed line: undamped panel – blue solid line: damped panel

Table 3: Overall value of the FRFs for door panels.

	0-100 (Hz)	0-200 (Hz)	0-400 (Hz)
Original (dB)	106,1	117,8	123,4
Damped (dB)	103,0	110,8	115,1

6 Conclusions

Structural material properties have been determined by the Oberst beam technique, a database which permits reliable reproduction of experimental tests by a FE model has been defined. Both pure CFRP structures and sandwich structures formed by CRFP and a damping material have been tested in the temperature range -20/+60 °C to evaluate the variability of the Young's modulus and the loss factor. A couple of CFRP automotive components, a leaf spring and the external panel of a door, have been manufactured and tested. The comparison of the experimental modal analysis with the results of the FE models revealed the two extreme important aspects. Not only the material has to be correctly defined but also a precise geometry of the FE model should be created to achieve a good correlation: even small geometrical variations, especially in curved and large surfaces, can lead to significant differences for dynamic responses. The influence of damping material has experimentally been verified and quantified on the door panel. A thin layer of KRAIBON® SUT9609/24 damping material has been embedded in the stacking sequence of the panel, with very limited impact on both the production process and the final cost of the component. The weigh variation of the panel is within +7% but its dynamic response dramatically improved with potentially significant effects on the noise harshness of the car interior environment.

Acknowledgments

The authors wish to acknowledge: Altair-Italy Engineering S.R.L. for providing the FE software and Gummiwerk KRAIBURG GmbH for the damping material "KRAIBON® SUT9609/24" and the active support during all the activity.

The authors declare that there is no conflict of interest regarding the publication of this paper.

References

[1] M. Carello and A. G. Airale, "Composite Suspension Arm Optimization for the City Vehicle XAM 2.0," in *Design and Computation of Modern Engineering Materials*, vol. 54, A. Öchsner and H. Altenbach, Eds. Cham: Springer International Publishing, 2014, pp. 257–272.

[2] M. Carello, A. Airale, A. Ferraris, and A. Messana, "XAM 2.0: from Student Competition to Professional Challenge," *Comput.-Aided Des. Appl.*, vol. 11, no. sup1, pp. S61–S67, May 2014.

[3] M. Carello, A. G. Airale, and A. Ferraris, "City Vehicle XAM 2.0: Design and Optimization of the Composite Suspension System," 2014.

[4] G. Brusaglino, Giuseppe Buja, Massimiliana Carello, Antonio Paolo Carlucci, Christopher H. Onder, and Monica Razzetti, "New technologies demonstrated at Formula Electric and Hybrid Italy 2008."

[5] H. Wan, Y. Li, and L. Zheng, "Vibration and Damping Analysis of a Multilayered Composite Plate with a Viscoelastic Midlayer," *Shock Vib.*, vol. 2016, pp. 1–10, 2016.

[6] "Standard Test Method for Measuring Vibration-Damping Properties of Materials," ASTM International, 2010.

[7] G. Erdoğan, F. Bayraktar, and K. Y. Sanliturk, "MEASUREMENT OF DYNAMIC PROPERTIES OF MATERIALS."

[8] "J1637: Laboratory Measurement of the Composite Vibration Damping Properties of Materials on a Supporting Steel Bar - SAE International." [Online]. Available: http://standards.sae.org/j1637_201306/. [Accessed: 22-Mar-2017].

[9] N. M. M. Maia and J. M. Montalvão e Silva, Eds., *Theoretical and experimental modal analysis*. Taunton, Somerset, England : New York: Research Studies Press ; Wiley, 1997.

[10] D. J. Ewins, *Modal testing: theory, practice, and application*, 2nd ed. Baldock, Hertfordshire, England ; Philadelphia, PA: Research Studies Press, 2000.

[11] E. Gandino, L. Garibaldi, and S. Marchesiello, "Covariance-driven subspace identification: A complete input–output approach," *J. Sound Vib.*, vol. 332, no. 26, pp. 7000–7017, Dec. 2013.

[12] B. Peeters, H. Van der Auweraer, P. Guillaume, and J. Leuridan, "The PolyMAX Frequency-Domain Method: A New Standard for Modal Parameter Estimation?," *Shock Vib.*, vol. 11, no. 3–4, pp. 395–409, 2004.

[13] J. Wang, C. Wang, T. Zhang, and B. Zhong, "Comparison of Different Independent Component Analysis Algorithms for Output-Only Modal Analysis," *Shock Vib.*, vol. 2016, pp. 1–25, 2016.

[14] A. Fasana, "Modal parameters estimation in the Z-domain," *Mech. Syst. Signal Process.*, vol. 23, no. 1, pp. 217–225, Jan. 2009.

[15] A. Fasana, M. Carello, A. Ferraris, A. Airale, and D. B. Polato, "NVH Analysis of Automotive Components: A Carbon Fiber Suspension System Case," in *Advances in Italian Mechanism Science*, vol. 47, G. Boschetti and A. Gasparetto, Eds. Cham: Springer International Publishing, 2017, pp. 345–354.

[16] K. Shin and J. K. Hammond, *Fundamentals of signal processing for sound and vibration engineers*. Chichester, England ; Hoboken, NJ: John Wiley & Sons, 2008.

[17] Altair Engineering, *Altair engineering: Practical aspect of Finite Element Simulation,* 3rd ed. 2015.

[18] Altair Engineering, *Altair engineering: Pre & post – processing for Finite Element Analysis, guidebook,*. 2015.

[19] Shashikant T. More and Dr. R. S. Bindu, "Effect of Mesh Size on Finite Element Analysis of Plate Structure," pp. 181–185, 03-May-2015.

[20] J. Rydh, "Very Large Symmetric Eigenvalue Problems Solved by Lanczos and Multiple Relatively Robust Representations for Tridiagonals," KTH.

[21] "Combining automated multilevel substructuring and subspace iteration for huge gyroscopic eigenproblems," *ResearchGate*. [Online]. Available: https://www.researchgate.net/publication/259193426_Combining_automated_multilevel_substructuring_and_subspace_iteration_for_huge_gyroscopic_eigenproblems. [Accessed: 25-Mar-2017].